Peculiarities in light scattering by spherical particles with radial anisotropy

Cheng-Wei Qiu[1,*] and Boris Luk'yanchuk[2]

[1]*Department of Electrical and Computer Engineering, National University of Singapore, 4 Engineering Drive 3, Singapore 117576*
[2]*Data Storage Institute, Agency for Science, Technology and Research, DSI Building, 5 Engineering Drive 1, Singapore 117608*
Corresponding author: eleqc@nus.edu.sg

Light scattering by a spherical particle with radial anisotropy is discussed by extending Mie theory to diffraction by an anisotropic sphere, including both the electric and the magnetic anisotropy ratio. It is shown that radial anisotropy may lead to great modifications in scattering efficiencies and field enhancement, elucidating the importance of anisotropies in the control of scattering. The capacity for nondissipating damping is demonstrated for anisotropic spheres with different signs in radial and transversal permittivities. © 2008 Optical Society of America

OCIS codes: 050.1940, 000.3860, 160.1190, 250.5403, 290.1350.

1. INTRODUCTION

The majority of solid materials in nature are anisotropic; e.g., polar crystallites made of orientational molecules are generally both anisotropic and collective. The presence of anisotropy is due to the lack of symmetry in the local atomic environment, and the collectivity is caused by the dense grouping of molecules. Understanding the role of these effects in light scattering is of particular interest for many medical and bioengineering applications. Most previous investigations into the ordering of orientational molecules and fluids have focused on 1D and 2D periodic substrates [1]. These problems have also been analyzed theoretically in terms of Landau theory [2] and Monte Carlo simulation [3]. Recently, the orientational ordering of colloidal molecules on 2D periodic substrates has been investigated both theoretically and numerically [4]. A few numerical approaches for 3D molecular-dynamics calculations have been reported [5,6]. However, the macroscopic anisotropic response of a spherical particle made of crystallites on the Maier–Saupe model has received less attention in spite of its importance in the technologies of the embedding of artificial particles and biomedical detection. Radially anisotropic materials have been receiving great attention recently from both the scientific and the engineering communities. It has been reported that the spherical or cylindrical cloak can be realized by a material with radial anisotropy using coordination transformation [7–9]; these studies were presented primarily in the optics limit or static cases. Thus, an analytical method is necessary to exactly characterize the wave interaction and to provide more physical insight into the design process of cloaking structures. The nonlinear physics of the material studied in this report has been investigated [10], where the nonlinear enhancement in second-harmonic and induced third-harmonic generation is found to be much larger than that of the corresponding isotropic systems.

Especially in medical applications and bioengineering, light scattering yields insight into the details of the interaction of embedded or injected bioparticles with microwave and/or optical illumination [11]. Scattering helps, for example, to locate some abnormal proteins. Of special interest are spherical particles with radial anisotropies. It is expected that molecules in spherical particles are at least partially oriented with respect to the direction normal to the surface. Such orientation of molecules can be easily included into the theory by considering the particle as a uniaxial anisotropic medium with the principal optic axis along with local direction normal to the surface. The complex dielectric and magnetic tensorial components ϵ_n (μ_n) and ϵ_t (μ_t) correspond to the field vectors normal to and tangential to the local surface (local optic axis [12]), respectively. This problem can be investigated systematically on the basis of the exact solution of the Maxwell equations, which demonstrates the extension of Mie theory to diffraction by an anisotropic sphere, including both the electric and the magnetic anisotropy ratio.

Some peculiarities in light scattering from isotropic materials were found recently for the case of weakly dissipating materials near plasmon resonance frequencies. For these isotropic materials, the classical Rayleigh scattering does not hold and can be replaced by anomalous light scattering [13]. This anomalous light scattering is associated with complex patterns of near and far fields, in contrast to Rayleigh scattering. It also demonstrates an extraordinary scattering effect [14], which is similar to quantum scattering by a potential with quasi-discrete levels exhibiting Fano resonances [15]. Another interesting effect refers to active random isotropic media, which support optical light enhancement [16]. Recently, scattering of light by anisotropic materials has been analyzed in [17–19], but the material is characterized primarily in rectangular coordinates and treated by a differential

theory. Therefore, the purpose of this paper is the analysis of the radial anisotropy effect upon the plasmonics and other extraordinary effects on the basis of an exact and compact solution for light scattering by spherical particles with uniaxial anisotropy defined in spherical coordinates.

2. FORMULATION

The sphere with uniaxial anisotropy is illuminated by a plane wave with the electric field polarized along the x axis. The constitutive tensors of the relative permittivity and permeability are defined as

$$\bar{\epsilon} = \begin{pmatrix} \epsilon_n & 0 & 0 \\ 0 & \epsilon_t & 0 \\ 0 & 0 & \epsilon_t \end{pmatrix}, \quad \bar{\mu} = \begin{pmatrix} \mu_n & 0 & 0 \\ 0 & \mu_t & 0 \\ 0 & 0 & \mu_t \end{pmatrix}, \tag{1}$$

where ϵ_n (or μ_n) and ϵ_t (or μ_t) stand for the permittivity (or permeability) elements corresponding to the electric (or magnetic)-field vector normal to and tangent to the local optic axis, respectively.

In [20], it has been proved that in radial anisotropic material the TE and TM waves are decoupled if off-axis elements are zero. Hence, solving the Maxwell equations using two Debye potentials, one has

$$\frac{\epsilon_n}{\epsilon_t}\frac{\partial^2 \Phi_{\mathrm{TM}}}{\partial r^2} + \frac{1}{r^2 \sin\theta}\frac{\partial}{\partial\theta}\left(\sin\theta\frac{\partial \Phi_{\mathrm{TM}}}{\partial\theta}\right) + \frac{1}{r^2 \sin^2\theta}\frac{\partial^2 \Phi_{\mathrm{TM}}}{\partial\phi^2}$$

$$+ \frac{\omega^2}{c^2}\epsilon_n\mu_t \Phi_{\mathrm{TM}} = 0, \tag{2}$$

$$\frac{\mu_n}{\mu_t}\frac{\partial^2 \Phi_{\mathrm{TE}}}{\partial r^2} + \frac{1}{r^2 \sin\theta}\frac{\partial}{\partial\theta}\left(\sin\theta\frac{\partial \Phi_{\mathrm{TE}}}{\partial\theta}\right)$$

$$+ \frac{1}{r^2 \sin^2\theta}\frac{\partial^2 \Phi_{\mathrm{TE}}}{\partial\phi^2} + \frac{\omega^2}{c^2}\epsilon_t\mu_n \Phi_{\mathrm{TE}} = 0. \tag{3}$$

Here we define the parameters of the anisotropy ratio: $A_e = \epsilon_t/\epsilon_n$ (electric-type) and $A_m = \mu_t/\mu_n$ (magnetic-type). Equations (2) and (3) convert into the usual wave equations for isotropic materials (see [12]). Electromagnetic fields can be expressed through those potentials. Solving these equations with the corresponding boundary conditions, one can find normalized scattering amplitudes a_l (electric) and b_l (magnetic)

$$a_l = \frac{\mathfrak{R}_l^{(a)}}{\mathfrak{R}_l^{(a)} + i\mathfrak{J}_l^{(a)}}, \quad b_l = \frac{\mathfrak{R}_l^{(b)}}{\mathfrak{R}_l^{(b)} + i\mathfrak{J}_l^{(b)}}, \tag{4}$$

where

$$\mathfrak{R}_l^{(a)} = n_t\psi_l'(q)\psi_{v_1}(n_tq) - \mu_t\psi_l(q)\psi_{v_1}'(n_tq), \tag{5}$$

$$\mathfrak{J}_l^{(a)} = n_t\chi_l'(q)\psi_{v_1}(n_tq) - \mu_t\chi_l(q)\psi_{v_1}'(n_tq), \tag{6}$$

$$\mathfrak{R}_l^{(b)} = n_t\psi_l(q)\psi_{v_2}'(n_tq) - \mu_t\psi_l'(q)\psi_{v_2}(n_tq), \tag{7}$$

$$\mathfrak{J}_l^{(b)} = n_t\chi_l(q)\psi_{v_2}'(n_tq) - \mu_t\chi_l'(q)\psi_{v_2}(n_tq). \tag{8}$$

Here $n_t = \sqrt{\epsilon_t\mu_t}$ is the complex refractive index, and the functions $\psi_v(x)$ and $\chi_l(x)$ are given by $\psi_v(x) = \sqrt{\pi x/2}J_{v+1/2}(x)$ and $\chi_l(x) = \sqrt{\pi x/2}N_{l+1/2}(x)$, respectively. The primes indicate differentiation with respect to the entire argument. The value $q = k_0a$ presents the so-called Mie size parameter, and a is the particle radius. One can see from these formulas that all the information about particle anisotropy is presented by the order of the spherical Bessel functions, i.e., $v_1 = \sqrt{l(l+1)A_e + 1/4} - 1/2$ and $v_2 = \sqrt{l(l+1)A_m + 1/4} - 1/2$, which can be derived from the general results in [20] by letting the off-axis parameters be zero. The radius a of the anisotropic sphere is fixed at $30\,\mu m$. In practical detection problems, the so-called radar backscattering cross section (RBSC) is of great interest. Those scattering efficiencies are the basis for further numerical analysis.

3. NUMERICAL ANALYSIS OF PECULIAR SCATTERING

A. Effects of the Anisotropy Ratio
In Fig. 1, we present the dependence of the backscattering efficiency (normalized by the geometric cross section πa^2) versus the size parameter of the particle with a single anisotropy ratio (SAR). Curves 1, 2, and 3 reveal the role of anisotropy in the scattering of normal anisotropic spheres, where limiting backscatterings are found for sufficiently high incident frequency. Interestingly, it is found that the backscattering would be significantly enhanced if the real part of electric SAR were negative. Also, it is noted that in a case such as curve 4, the oscillation will exist in a wider band of frequency, resulting in no constant values. Given the physical size of the radius, one can sweep the incident frequency and judge from the signal strengths on the receiver to differentiate those special
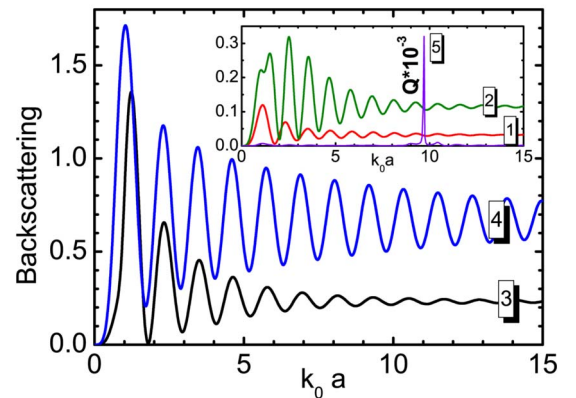

Fig. 1.   (Color online) Normalized backscattering efficiency versus k_0a at the same scale of radial oscillation where only electric anisotropy ratio is present. $\mu_n = \mu_t = 1 + 0.2i$ and $\epsilon_n = 2 + 0.6i$ are assumed for all curves. Curve 1 (red): $\epsilon_t = 2 + 0.6i$ ($A_e = 1$). Curve 2 (olive): $\epsilon_t = 4 + 1.2i$ ($A_e = 2$). Curve 3 (black): $\epsilon_t = 8 + 2.4i$ ($A_e = 4$). Curve 4 (blue): $\epsilon_t = -4 + 1.2i$ ($A_e = -1.67 + 1.1i$). Curve 5 (violet): $\epsilon_t = -4 - 1.2i$ ($A_e = -2$). Curve 1 corresponds to the isotropic case. In curve 5, one can see light enhancement in anisotropic spheres at 15.44 THz (i.e., the size parameter at 9.7), and the amplitude of backscattering is shown with normalization factor of 10^{-3} (i.e., maximal amplitude is above 300).

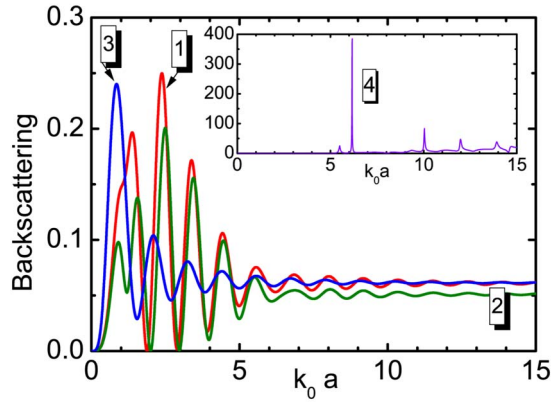Fig. 2.   (Color online) Normalized backscattering efficiency with joint anisotropy ratios of A_e and A_m. The same radial oscillation is assumed, $\epsilon_n = 2 + 0.6i$, for all curves. Curve 1 (red): $\epsilon_t = 4 + 1.2i$ ($A_e = 2$), $\mu_r = 1 + 0.2i$, $\mu_t = 1.5 + 0.3i$ ($A_m = 1.5$). Curve 2 (olive): $\epsilon_t = 3.76 + 1.2i$ ($A_e = 2 + 0.4i$), $\mu_r = 1 + 0.2i$, $\mu_t = 1.5 + 0.3i$ ($A_m = 1.5$). Curve 3 (blue): $\epsilon_t = -4 + 1.2i$ ($A_e = -1.67 + 1.1i$), $\mu_r = 1 + 0.2i$, $\mu_t = -1.5 + 0.3i$ ($A_m = -1.38 + 0.58i$). Curve 4 (violet): $\epsilon_t = -4 - 1.2i$ ($A_e = -2$), $\mu_r = 1 + 0.2i$, $\mu_t = -1.5 - 0.3i$ ($A_m = -1.5$). For the last case, one can see light enhancement in active materials with negative refractive index at 9.8 THz, i.e., size parameter at 6.16. Several enhanced backscatterings also exist at other frequencies.

molecules having negative electric SAR within a molecular ensemble. The inset in Fig. 1 further illustrates the sophisticated variation in a more detailed range. Of particular interest is the case of curve 5, where the light enhancement is observed. Thus, a small anisotropic object may be regarded as if it has a large physical cross section. However, such giant enhancement is quite sensitive to the incident frequency.

In Fig. 2 the effects of the joint anisotropy ratio (JAR) are examined so as to demonstrate how the backscattering is affected by the simultaneous presence of A_e and A_m. Analogously, the oscillations in the backscattering for JAR are found to be convergent versus the size parameter. Comparing curve 1 with curve 3, one can see that the opposite signs in the real parts of the transverse parameters (ϵ_t and μ_t) would lead to the same limiting value of

the backscattering, but the scattering patterns for small size parameters are dramatically modified. The enhanced light scattering of JAR has a more complex pattern than that of SAR. Multiple resonances can be found in JAR cases with the strongest one located at 9.8 THz, the second strongest at 16.07 THz, and some smaller ones.

Figure 3 shows the dependence of the backscattering on the anisotropy ratio. It is found that the variation of the backscattering is more sensitive to the transverse oscillation. In Fig. 3(b), the suppression of the backscattering of a small anisotropic particle arises only in the range $0 < \epsilon_n < 1$, depending on the size parameter. However, the variation of the backscattering will be complicated when the radial oscillation is fixed and transverse oscillation is tuned. In particular, for the red curve (curve 2) in Fig. 3(a), there are two critical values of ϵ_t corresponding to the backscattering suppression (one within $0 < \epsilon_n < 1$ and the other in the vicinity of $\epsilon_n = 6.5$). This implies that the energy stored in the transverse and radial directions is reversible if the anisotropy ratio is properly manipulated, resulting in extraordinary scattering diagrams.

B. Nondissipative Damping
The situation where the transverse (ϵ_t) and the radial (ϵ_n) permittivities have opposite signs is of special interest. In Fig. 4, one can see quite an unusual effect when the particle is "plasmonic" ($\epsilon_t < -2$) in the transverse direction and "dielectric" ($\epsilon_n > 1$) in the radial direction. Although the material is nondissipative (Im[ϵ]=0 for all cases), one can see that $Q_{sca} \neq 0$ (with the maximum near $q \approx 1.5$). In principle, the damping of an electromagnetic field during its propagation in a nondissipative medium is not forbidden in physics. For instance, Landau damping exists in a collisionless plasma [21]. The formal mathematical reason for Landau damping is related to properties of some contour integral, and the physical reason lies in the resonant absorption of the energy of Langmuir waves by electrons whose velocity coincides with the phase velocity of
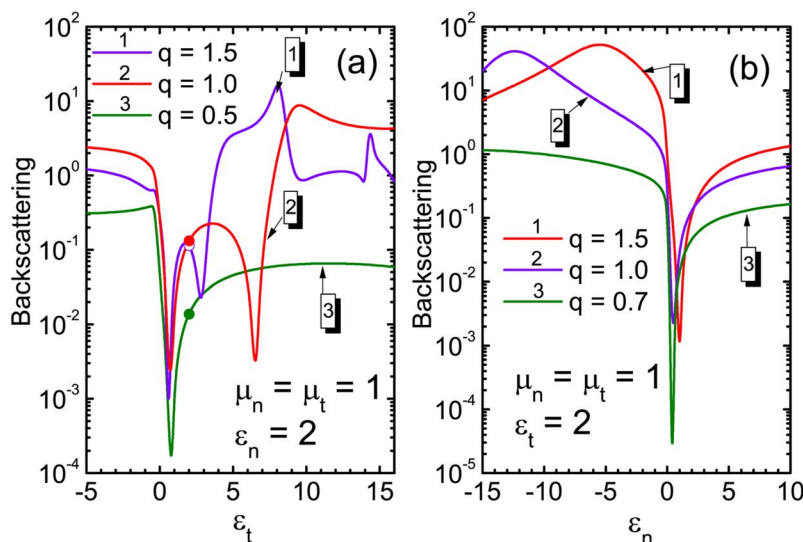

Fig. 3.   (Color online) Variation of backscattering efficiency versus electric anisotropy. Points in (a) refer to the isotropic case. Radial and transverse oscillations are kept unchanged, respectively, in (a) and (b).
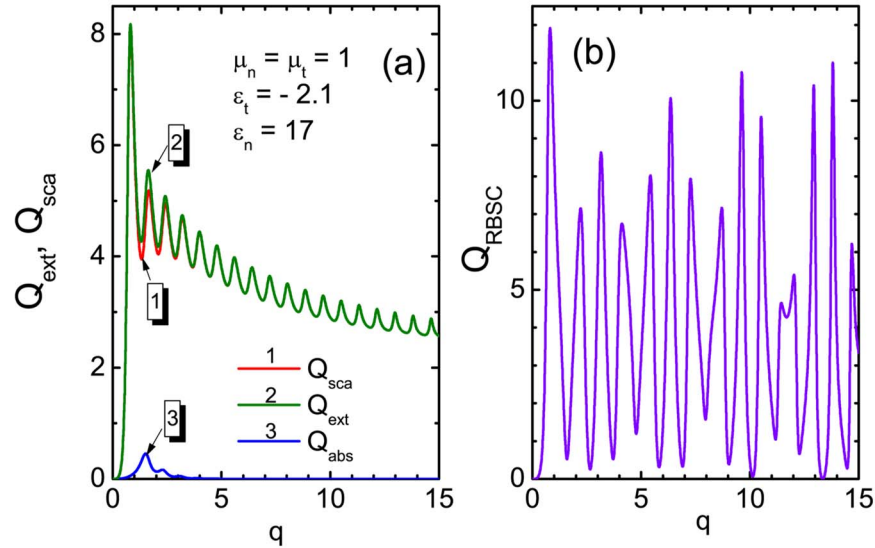
Fig. 4.   (Color online) Scattering efficiencies for nondissipative anisotropic spheres with strong radial oscillation where the nondissipative damping arises: (a) nonzero absorption cross section for nondissipative anisotropic particles; (b) highly oscillating backscattering cross section when the nondissipative damping occurs. The radial oscillation is assumed to be $\epsilon_n = 17$, and the transverse oscillation $\epsilon_t = -2.1$ is near surface-plasmon resonance. It shows that the damping arises within a certain frequency range even for a nondissipative anisotropic sphere that has a strong radial oscillation and a transverse oscillation near the surface-plasmon resonance.

the waves. In the case of light scattering, one should remember that the dissipation arises due to $\mathrm{Im}[\epsilon_{n,t}] > 0$ and (or) $\mathrm{Im}[\mu_{n,t}] > 0$, as follows from the Maxwell equations (see, e.g., [22]). Thus, with all $\mathrm{Im}[\epsilon_{n,t}] = \mathrm{Im}[\mu_{n,t}] = 0$, we have no "true dissipation." In the case of isotropic nondissipative materials, it yields $Q_{abs} \equiv 0$. Formally, it follows from the properties of the Bessel and Neumann functions with the real order l, which gives the real values to $\mathfrak{R}$ and $\mathfrak{I}$ in the form of $\mathfrak{R}/(\mathfrak{R}+i\mathfrak{I})$ for those amplitudes in Eq. (4). In such conventional cases, the identity $Q_{sca} \equiv Q_{ext}$ i.e., $Q_{abs} \equiv 0$, automatically holds, because $\mathrm{Re}[\mathfrak{R}/(\mathfrak{R}+i\mathfrak{I})] \equiv |\mathfrak{R}/(\mathfrak{R}+i\mathfrak{I})|^2 \equiv \mathfrak{R}^2/(\mathfrak{R}^2+\mathfrak{I}^2)$. This property still exists in anisotropic materials when A_e and A_m are positive and the orders (i.e., v_1 and v_2) are also positive and real.

However, the orders of the Bessel functions become imaginary numbers if the anisotropy ratio is negative, resulting in exotic behavior of the Bessel functions. These Bessel functions are still analytical functions, which contain both real and imaginary parts. Thus, the scattering amplitudes have the form $(\mathfrak{R}_1+i\mathfrak{R}_2)/(\mathfrak{R}_1+i\mathfrak{R}_2+i\mathfrak{I}_1-\mathfrak{I}_2)$, where $\mathfrak{R}_{1,2}$ and $\mathfrak{I}_{1,2}$ are real valued. For these scattering amplitudes, the condition of $\mathrm{Re}[a] \equiv |a|^2$ does not hold, i.e., $Q_{abs} \neq 0$, which can be seen in Fig. 4.

In the case of Landau damping, each electron emits exactly the same energy that it absorbs, and thus the averaged value of the energy absorbed by each electron is equal to zero (no dissipation). However, collisionless plasma with many electrons moving with different velocities leads to damping of the amplitude of the propagating wave due to the noncoordinated absorption–emission processes of different electrons. It is not the "true dissipation" shown in Fig. 4, and the energy is reversibly stored "somewhere" in this anisotropic media like electromagnetic energy stored in an inductance-capacitance network circuit. Such effects can be presented, e.g., in the form of

plasma echo. In the case of light scattering by the anisotropic particle studied, the energy is redistributed within the electromagnetic modes, which produces the eigenmodes of the particle. These modes also can absorb and emit electromagnetic energy.

We have discussed in this paper the mathematical reason for the deviation in scattering and extinction efficiencies [when $l(l+1)A_e + 1/4 < 0$, the order of the Bessel function $\sqrt{l(l+1)A_e + 1/4} - 1/2$ becomes a complex number, resulting in a nonzero imaginary part in the value of the Bessel function]. This means that corresponding oscillations have phase shifts and the emission/absorption process occurs with different time delays for different modes. Although each partial oscillation has no dissipation, the resulting summary oscillation looks like damping in the scattering because of the noncoordinated absorption/emission processes of different modes with different phase shifts.

The problem of light storage in the isotropic particles has been discussed previously in a number of papers, e.g., [23]. Particles with radial anisotropy thus suggest a new idea for this light storage because of the anisotropy. The anisotropic particle represents an even more special situation since the oscillation is disturbed by the anisotropy in a complex way, especially when the radial permittivity is high and transverse permittivity seems "plasmonic" as in Fig. 4. Thus, if we compare such an anisotropic case with the isotropic case, the idea is to consider the averaged permittivity of the anisotropic particle in which electron velocities have a Maxwellian distribution function. Hence, the averaged permittivity will possess a "virtual" imaginary part, resulting in the nondissipative absorption, as reported.

From Fig. 4, we further find that when the transverse permittivity is near surface-plasmon resonance and the radial oscillation is strong, highly oscillative radar back-
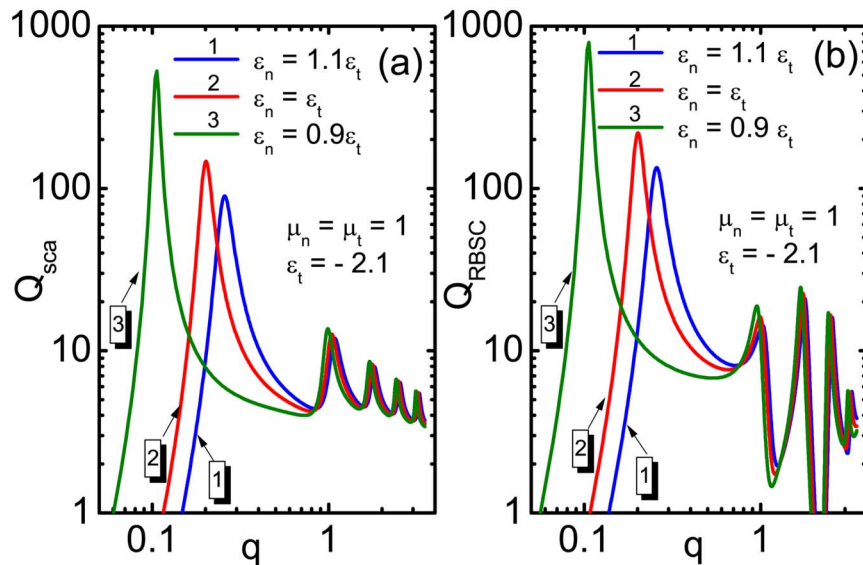
Fig. 5.   (Color online) Scattering efficiencies for nondissipative anisotropic spheres near surface-plasmon resonance. Both radial and transversal oscillations are near surface-plasmon resonance, and three electric anisotropy ratios (i.e., $A_e < 1$, $A_e = 1$, and $A_e > 1$) are particularly studied to demonstrate the significance of anisotropy in (a) scattering cross section and (b) backscattering cross section when the anisotropic particles are near surface-plasmon resonance.

scattering (Q_{RBSC}) occurs. This implies that the wave dissipates when the stored energy is reversed between absorption and emission. A fine change in the incident frequency (i.e., size parameter) will result in significant variation in backscattering, and at certain frequencies even zero backscattering can be realized.

Nondissipative anisotropic spheres near surface-plasmon resonances, with a slight anisotropy, are also investigated [12]. In such circumstances, it is found that the plasmon resonance can be tuned by changing the velocities and directions of electron movements along the radial direction. The red curve (curve 2) in Fig. 5 denotes the isotropic case near surface-plasmon resonance. However, even though the electron movement along the radial oscillation is modified slightly, the scattering efficiencies will be changed drastically for small particles. Figure 5 also shows that electric anisotropy larger than unity (i.e., $A_e > 1$) favors the scattering enhancement particularly for nanoscaled particles. When the size parameter approaches a sufficiently large value, the role of aniostropy becomes negligible.

4. SUMMARY

In summary, anomalous scatterings of spherical particles with radial anisotropies are studied by an exact solution to take into account the anisotropy effects. The role of the anisotropy ratio, both electric and magnetic, is discussed in the control of scattering. If the anisotropy ratio is configured properly, small objects can be "observable" and (or) "transparent" to external detecting devices. Peculiar backscatterings are presented with physical insights. Since abnormal membranes usually have much higher adhesive ability than normal ones, the theory proposed here would be very meaningful in the biomedical detection of those abnormal proteins if future biotechnology makes it easier to arrange the deposits of such implanted orientational molecules so as to induce a desirable aniso-

tropy ratio. Moreover, for the practical engineering of radar detection, the present work also provides insights into how to design the coating for aircraft and how to make use of the SAR and JAR to minimize or enhance radar cross sections if unintentional anisotropy is introduced by natural causes or by the shear in the surface plane during processing.

REFERENCES

1. D. R. Nelson, *Phase Transitions and Critical Phenomena* (Academic, 1983).
2. S. Alexander and J. McTague, "Should all crystals be bcc? Landau theory of solidification and crystal nucleation," Phys. Rev. Lett. **41**, 702–705 (1978).
3. J. Chakrabarti, H. R. Krishnamurthy, A. K. Sood, and S. Sengupta, "Reentrant melting in laser field modulated colloidal suspensions," Phys. Rev. Lett. **75**, 2232–2235 (1995).
4. C. Reichhardt and C. J. Olson, "Novel colloidal crystalline states on two-dimensional periodic substrates," Phys. Rev. Lett. **88**, 248301 (2002).
5. J. D. Johnson, M. S. Shaw, and B. L. Holian, "The thermodynamics of dense fluid nitrogen by molecular dynamics," J. Chem. Phys. **80**, 1279–1294 (1984).
6. L. Joly, C. Ybert, E. Trizac, and L. Bocquet, "Hydrodynamics within the electric double layer on slipping surfaces," Phys. Rev. Lett. **93**, 257805 (2004).
7. J. B. Pendry, D. Schurig, and D. R. Smith, "Controlling electromagnetic fields," Science **312**, 1780–1782 (2006).
8. D. Schurig, J. B. Pendry, and D. R. Smith, "Calculation of material properties and ray tracing in transformation media," Opt. Express **14**, 9794–9804 (2006).
9. S. A. Cummer, B. I. Popa, D. Schurig, D. R. Smith, and J. B. Pendry, "Full-wave simulations of electromagnetic cloaking structures," Phys. Rev. E **74**, 036621 (2006).

10. L. Gao and X. P. Yu, "Second- and third-harmonic generations for a nondilute suspension of coated particles with radial dielectric anisotropy," Eur. Phys. J. B **55**, 403–409 (2007).
11. M. F. Yanik, H. Cinar, H. N. Cinar, A. D. Chisholm, Y. Jin, and A. Ben-Yakar, "Neurosurgery functional regeneration after laser axotomy," Nature **432**, 822–822 (2004).
12. B. S. Luk'yanchuk and C. W. Qiu, "Enhanced scattering efficiencies in spherical particles with weakly dissipating anisotropic materials," Appl. Phys. A (2008), doi: 10.1007/s00339-008-4572-5.
13. M. I. Tribelsky and B. S. Luk'yanchuk, "Anomalous light scattering by small particles," Phys. Rev. Lett. **97**, 263902 (2006).
14. B. S. Luk'yanchuk, M. I. Tribelsky, Z. B. Wang, Y. Zhou, M. H. Hong, L. P. Shi, and T. C. Chong, "Extraordinary scattering diagram for nanoparticles near plasmon resonance frequencies," Appl. Phys. A **89**, 259–264 (2007).
15. M. I. Tribelsky, S. Flach, A. E. Miroshnichenko, A. V. Gorbach, and Y. S. Kivshar, "Light scattering by a finite obstacle and Fano resonances," Phys. Rev. Lett. **100**, 043903 (2008).
16. P. Bermel, E. Lidorikis, Y. Fink, and J. D. Joannopoulos, "Active materials embedded in photonic crystals and coupled to electromagnetic radiation," Phys. Rev. B **73**, 165125 (2006).
17. B. Stout, M. Nevière, and E. Popov, "Mie scattering by an anisotropic object. Part I. Homogeneous sphere," J. Opt. Soc. Am. A **23**, 1111–1123 (2006).
18. B. Stout, M. Nevière, and E. Popov, "Mie scattering by an anisotropic object. Part II. Arbitrary-shaped object: differential theory," J. Opt. Soc. Am. A **23**, 1124-1134 (2006).
19. B. Stout, M. Nevière, and E. Popov, "T matrix of the homogeneous anisotropic sphere: applications to orientation-averaged resonant scattering," J. Opt. Soc. Am. A **24**, 1120–1130 (2007).
20. C. W. Qiu, L. W. Li, Q. Wu, and T. S. Yeo, "Field representations in general gyrotropic media in spherical coordinates," IEEE Antennas Wireless Propag. Lett. **4**, 467–470 (2005).
21. L. D. Landau, "On electron plasma oscillations," Sov. Phys. JETP **16**, 574 (1946) (in Russian).
22. L. D. Landau and E. M. Lifshitz, *Electrodynamics of Continuous Media* (Butterworth-Heinemann, 2002).
23. Z. M. Zhu, D. J. Gauthier, and R. W. Boyd, "Stored light in an optical fiber via stimulated Brillouin scattering," Science **318**, 1748–1750 (2007).